J. Cao and C. T.-C. Nguyen, "Drive Amplitude Dependence of Micromechanical Resonator Series Motional Resistance," *Digest of Technical Papers*, 10th International Conference on Solid-State Sensors and Actuators, Sendai, Japan, June 7-10, 1999, pp. 1826-1829.

Drive Amplitude Dependence of Micromechanical Resonator Series Motional Resistance

Jun Cao and Clark T.-C. Nguyen

Center for Integrated Micro Systems
Department of Electrical Engineering and Computer Science
University of Michigan, Ann Arbor, MI 48109-2122, U.S.A.

ABSTRACT

Frequency measurements are utilized to show that the series motional resistance R_x of a capacitive-comb transduced folded-beam micromechanical resonator depends strongly on drive amplitude when operated under vacuum. Subsequent measurements in air made via an electromechanical amplitude modulation (EAM) technique then contradict findings in vacuum, showing no R_x drive-level dependence when the resonator is operated under atmospheric pressure. Based on these results, a mechanism is tentatively proposed for low-pressure R_x drive-level dependence based primarily on Q variations with amplitude.

I. INTRODUCTION

Among the most interesting phenomena exhibited by oscillators referenced to high-Q, comb-driven micromechanical resonators ("μresonators") is their ability to amplitude limit without the need for nonlinearity in the active devices sustaining oscillation [1]. This behavior becomes possible when μmechanical resonator nonlinearity substitutes for amplifier nonlinearity, and can be advantageous because the noise figure of the sustaining amplifier is much smaller when it operates linearly than otherwise [2]. This in turn leads to enhanced performance in applications using μresonator oscillators, such as wristwatches or gyroscopes. Unfortunately, however, amplitude limiting via resonator nonlinearity is also often accompanied by oscillator instability under specific biasing conditions [1], making this method for amplitude limiting a somewhat dangerous prospect. Before it can be considered for use, then, a better understanding of the mechanism behind resonator-based amplitude limiting is required.

Pursuant to this, Section II in this paper first identifies a mechanism for oscillator limiting based upon a drive-level dependence of the series motional resistance R_x of comb-driven micromechanical resonators. A quantitative theoretical model for this phenomenon is then proposed and experimentally refined through characterization of air-damped μmechanical resonators in Sections III and IV via an electromechanical amplitude modulation (EAM) measurement technique.

II. DRIVE-LEVEL DEPENDENCE OF R_X

Figure 1 presents the scanning electron micrograph (SEM) of the polysilicon folded-beam μmechanical resonator used for this work. This resonator was fabricated using a two-mask surface micromachining process, in which the substrate serves as a blanket ground plane (electrically attached to the resonator itself), and drive/sense electrodes are elevated and electrically isolated from the substrate via oxide mesas. Figure 2 shows a frequency measurement scheme appropriate for vacuum environments, where the Q of the resonator exceeds 40,000. In this scheme, the resonator series LCR equivalent circuit [1] is in parallel with probe-to-probe feedthrough capacitance C_{PD}, yielding an overall equivalent circuit as shown in Fig. 3.

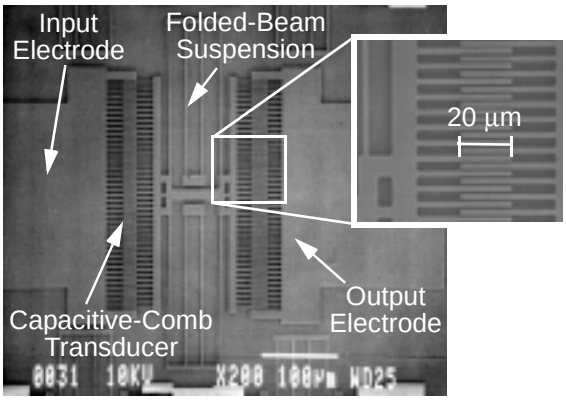

Fig. 1: SEM of an 18.21kHz polysilicon μmechanical resonator used for this work.

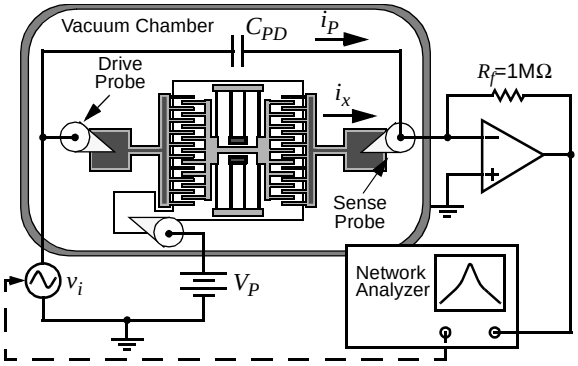

Fig. 2: Test apparatus used to measure the frequency characteristic of a μmechanical resonator operating under vacuum.

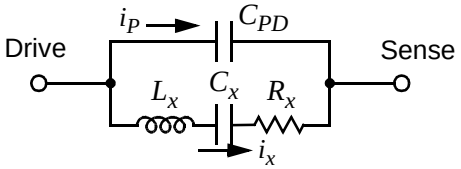

Fig. 3: Equivalent circuit for the resonator of Fig. 2.

Figure 4 presents frequency spectra for the μresonator of Fig. 1 measured under 50 mTorr vacuum using the circuit of Fig. 2 for increasing values of drive voltage v_i and with frequency normally swept upwards

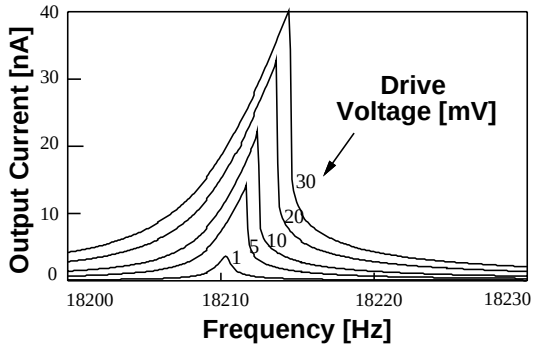

Fig. 4: Frequency characteristics for the μresonator of Fig. 1 measured under 50 mTorr vacuum for increasing drive voltage amplitudes.

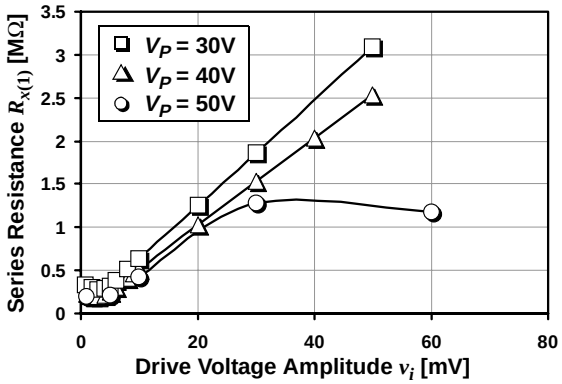

Fig. 5: Measured plot of R_x versus drive amplitude for the μresonator of Fig. 1 operated under 50μTorr pressure. (Displacements: 0-14 μm.)

so that the Duffing jump occurs at the true resonance point in overdriven cases. With data from Fig. 4, the series motional resistance as a function of drive-level can then be obtained via the expression

$$R_{x(1)} = \frac{v_i}{i_{x(1)}} = -\frac{R_f}{|v_{o(1)}/v_i|}, \qquad (1)$$

where R_f is indicated in Fig. 2, and $|v_{o(1)}/v_i|$ represents the magnitude of the input-to-output voltage transfer function of the electromechanical circuit in Fig. 2 evaluated at the highest point in the spectrum, whether Duffing distortion is present or not. The "(1)" subscript in Eq. (1) denotes the fundamental component of a given signal or a quantity derived from a fundamental signal component, needed for example in cases where nonlinearities generate distortion harmonics in certain signals. Applying data from Fig. 4 to (1) yields the $R_{x(1)}$ versus drive amplitude v_i curves of Fig. 5, plotted for various values of dc-bias V_P. Clearly, R_x exhibits a distinct dependence on drive amplitude when operated under vacuum, and it is this dependence that most likely governs the limiting behavior of μmechanical resonator oscillators [1].

Some insight into the mechanism behind the observed drive-level dependence can be obtained via consideration of the analytical expression for the R_x of a comb-driven μresonator with symmetrical ports, which can be written as [1]:

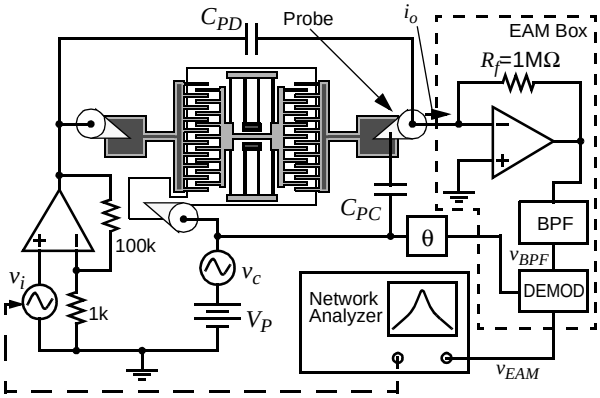

Fig. 6: Schematic of the EAM system for measuring the frequency spectra of low Q μmechanical resonators.

$$R_x = \frac{\omega_o m_r}{QV_P^2[2N_f(\partial C/\partial x)_{sov}]^2}, \qquad (2)$$

where ω_o and m_r are the (radian) resonance frequency and effective mass of the resonator at the shuttle location, respectively, $(\partial C/\partial x)_{sov}$ is the capacitance change per unit displacement for a single finger overlap, and N_f is the number of resonator fingers per comb-transducer. Of the parameters in (2), assuming a constant V_P, only Q and/or $(\partial C/\partial x)_{sov}$ can change appreciably with amplitude, so are most likely responsible for the observed drive level dependence.

To identify which of the two dominates, a measurement is needed in which one of the variables is constrained. Of the two, Q is the most convenient choice, since it can be constrained by merely operating the resonator at atmospheric pressure, where (for the resonator of Fig. 1) its Q drops from 43,000 to only 22 due to viscous gas damping [3], and maintains this value irrespective of drive amplitude.

Unfortunately, at atmospheric pressure, frequency spectra can no longer be obtained using the simple circuit of Fig. 2, since feedthrough currents from larger v_i's now overpower motional currents arising from the (now low Q) comb-transduced μmechanical resonator. In particular, at resonance, L_x and C_x cancel in the μresonator equivalent circuit, reducing it to just the resistor R_x. Thus, at resonance, R_x and C_{PD} compete to determine the total output current presented to the transresistance amplifier input. As Q decreases, R_x increases, and motional current i_x decreases to the point where currents feeding through C_{PD} dominate the output current response, effectively masking i_x and corrupting the μresonator frequency spectrum.

III. ELECTROMECHANICAL AMPLITUDE MODULATION (EAM)

To measure the motional current i_x from a low Q comb-driven μresonator, i_x must be separated from the parasitic feedthrough current i_P. For this purpose, an electromechanical amplitude modulation (EAM) measurement system shown in Fig. 6 [4] is used that separates motional currents from parasitics in the

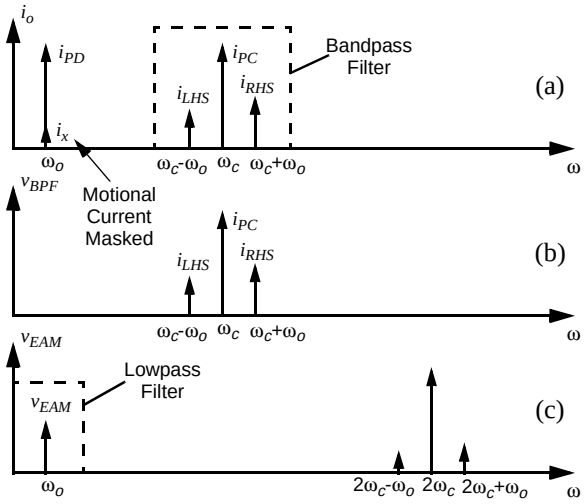

Fig. 7: Spectral density plots summarizing EAM post processing steps needed to attain an output voltage suitable for input to a network analyzer.

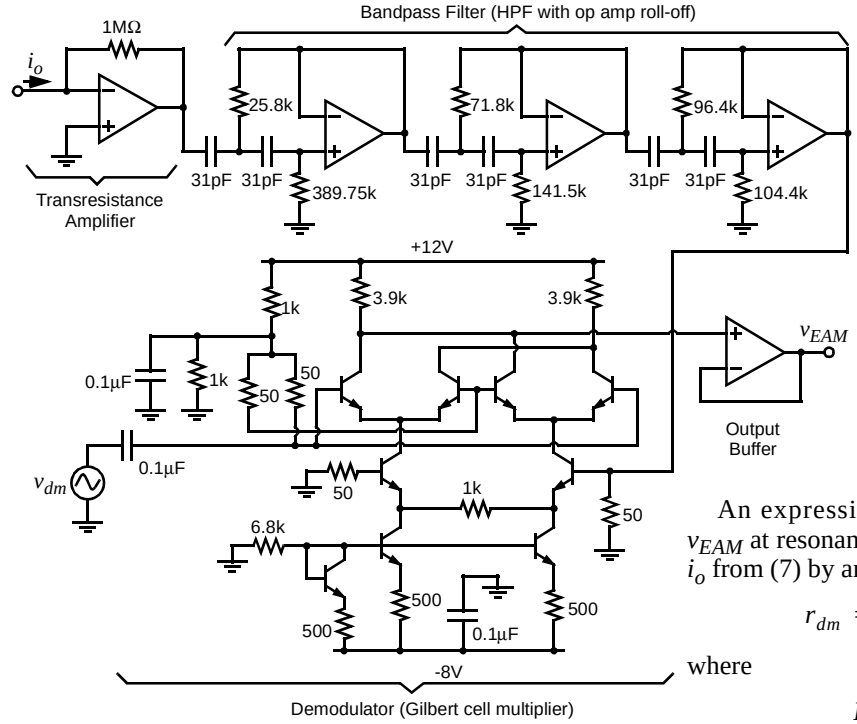

Fig. 8: Complete schematic for the circuit within the "EAM box" of Fig. 6.

frequency domain. As shown, this is achieved by simply adding a carrier signal v_c to the dc bias voltage V_P (which is normally applied to activate the capacitive-comb transducers [1]). Once v_c is added, the output current becomes (referring to Fig. 6)

$$i_o = C_{PD}\frac{dv_i}{dt} + C_{PC}\frac{dv_c}{dt} + C(t)\frac{dv_c}{dt} + (V_P + v_c)\frac{dC}{dt}, \quad (3)$$

where

$$v_i = V_i\cos\omega_i t \ , \ v_c = V_c\cos\omega_c t \quad (4)$$

$$C(t) = C_o + C_m\sin\omega t, \quad (5)$$

and [4]

$$C_m = \frac{k_r^{-1}V_P[2N_f(\partial C/\partial x)_{sov}]^2V_i}{1-(\omega/\omega_o)^2 + j(\omega/(Q\omega_o))} \quad (6)$$

where C_o is the static finger-to-finger overlap capacitance at the output port. Solving (3) at resonance, the current entering the summing node of the transimpedance amplifier at resonance reduces to

$$\begin{aligned} i_o = \ & i_P - \omega_o V_P C_m\cos\omega_o t \\ & -(1/2)(\omega_c-\omega_o)C_m V_c\cos(\omega_c-\omega_o)t \\ & +(1/2)(\omega_c+\omega_o)C_m V_c\cos(\omega_c+\omega_o)t \end{aligned} \quad (7)$$

where i_P represents components of current feeding through dc capacitors, C_{PD} and C_{PC}. Here, the resonator displacement now effectively amplitude modulates the carrier v_c, creating EAM motional current sidebands at frequencies (ω_c–ω_o) and (ω_c+ω_o). In this way, the motional current i_x is effectively separated from parasitic feedthrough currents that remain at ω_o.

Figure 7(a) plots the spectral density for the output current i_o directed to the input of the "EAM box". Once received, the "EAM box" then amplifies i_o via a transresistance amplifier, removes components at ω_o via a bandpass filter (Fig. 7(b)), then demodulates the EAM sidebands via a balanced Gilbert cell multiplier (Fig. 7(c)), generating a voltage signal in the vicinity of ω_o suitable for input to a network analyzer. The complete "EAM box" implementation, with all circuit element details, is presented in Fig. 8.

An expression for the EAM output voltage v_{EAM} at resonance can be obtained by multiplying i_o from (7) by an effective multiplier

$$r_{dm} = R_{dm}\cos(\omega_c t + \theta), \quad (8)$$

where

$$R_{dm} = R_f K_{mult}, \quad (9)$$

and where K_{mult} is the effective gain of the Gilbert cell multiplier. Multiplying (7) and (8) yields

$$v_{EAM} = i_o r_{dm} = V_{EAM}e^{\angle V_{EAM}}, \quad (10)$$

where

$$V_{EAM} = \frac{1}{2}C_m V_c R_{dm}\sqrt{\omega_o^2\cos^2\theta + \omega_c^2\sin^2\theta} \quad (11)$$

$$\angle V_{EAM} = \tan^{-1}\left(-\frac{\omega_c\sin\theta}{\omega_o\cos\theta}\right). \quad (12)$$

To maximize the output voltage of the EAM circuit at resonance, the demodulating sinusoid must be chosen with $\theta = 90^o$. A phase shifter is provided in the cir-

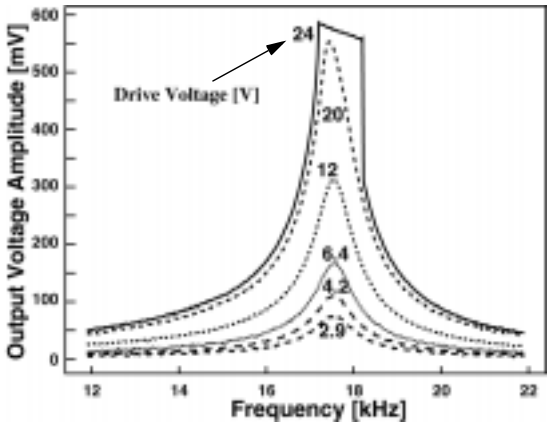

Fig. 9: Measured frequency characteristics for a 17.6kHz, folded-beam, comb-transduced μresonator measured under atmospheric pressure for varying values of drive amplitude v_i.

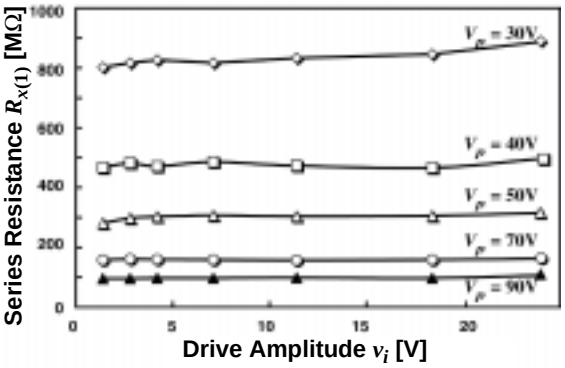

Fig. 10: Measured plot of R_x versus drive amplitude for a 17.6kHz μmechanical resonator operated under atmospheric pressure. (Displacements: 0-14 μm.)

cuit of Fig. 6 for this purpose.

IV. EXPERIMENTAL RESULTS

Figure 9 presents low Q spectra obtained in air for a 17.6 kHz comb-driven μmechanical resonator for increasing drive amplitudes and with frequency swept upwards using the EAM circuit summarized by Figs. 6 and 8. Again, these curves represent constant Q frequency characteristics for this μresonator, since the overall Q is constrained to ~22 by gas damping at atmospheric pressure. Data from these characteristics then yield the $R_{x(1)}$ versus drive amplitude curves plotted in Fig. 10. Clearly, R_x stays constant with drive amplitude under constant Q conditions, suggesting (in the absence of unexpected modes) that the R_x dependence on drive amplitude seen under vacuum arises from damping increases (or Q degradation) with drive amplitude, rather than $(\partial C/\partial x)$ (or transducer coupling) variations. Note also that the R_x's in the curves of Fig. 10 show a $1/V_P^2$-dependence that matches (2).

Applying data from Fig. 5 to (2) with measured values of $(\partial C/\partial x)_{sov}$ (on the order of ~14pF/m at low amplitudes), $\omega_o = 2\pi(18.21\text{kHz})$, $m_r = 5.73\times10^{-11}$ kg, and tentatively assuming that Q variations with displacement account for all R_x changes (i.e., $(\partial C/\partial x)$ assumed constant), Fig. 11 presents Q as a function of drive amplitude.

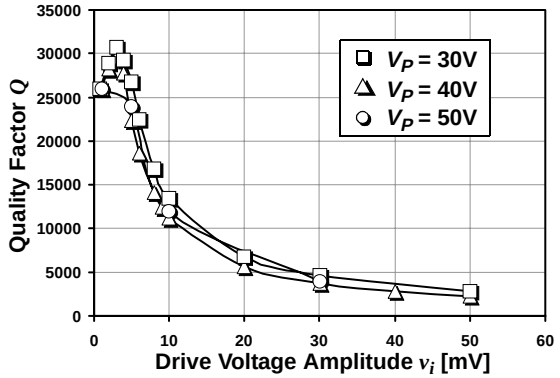

Fig. 11: Q versus drive amplitude plots for varying V_P's, determined with the assumption that $(\partial C/\partial x)$ remains constant with drive amplitude.

It should be stressed that the above data really only establishes that $(\partial C/\partial x)$ does not change with amplitude under low Q conditions; i.e., it does not necessarily establish that Q is entirely responsible for R_x drive-level dependence. In particular, under the high Q conditions where R_x dependence on drive-level is actually seen, $(\partial C/\partial x)$ dependence on drive-level is still quite possible. For example, a vertical component of motion seen only under vacuum that becomes larger with larger displacement amplitudes could reduce $(\partial C/\partial x)$ with drive amplitude, causing a corresponding increase in R_x. Such a mechanism might be damped out at atmospheric pressure, and thus, may not be discernible by air measurements. Thus, although a Q-based mechanism for R_x drive-level dependence seems likely, it is stated tentatively, pending further investigation.

V. CONCLUSIONS

The series motional resistance of a comb-driven micromechanical resonator has been observed to vary with drive level in vacuum, and this phenomenon is believed to allow amplitude limiting without active device nonlinearity in oscillators referenced to such resonators. Theoretical modeling predicts that this drive-level dependence derives from either Q or transducer coupling variations with amplitude. The fact that R_x drive-level dependence is not observed under atmospheric pressure (where Q is constrained) gives some evidence that Q variations with drive amplitude govern this phenomenon in vacuum. This is still a tentative result, however, as transducer coupling variations with amplitude cannot be eliminated as a mechanism, especially given the possibility of combined vertical/lateral resonance modes in vacuum.

Acknowledgment: This work was supported under grants from NSF and DARPA.

References:

[1] C. T.-C. Nguyen, *et al., IEEE J. Solid-State Circuits*, vol. 34, no. 4, pp. 440-445, April 1999.

[2] W. P. Robins, *Phase Noise in Signal Sources*. London: Peter Peregrinus, Ltd., 1982.

[3] Y.-H. Cho, *et al., J. Microelectromechan. Syst.*, vol. 3, no. 2, pp. 81-87, June 1994.

[4] C. T.-C. Nguyen, Ph.D. Dissertation, 1994.